ELSEVIER

Chemical Engineering Journal 120 (2006) 33–42

Chemical Engineering Journal

www.elsevier.com/locate/cej

Comparison between deactivation pattern of catalysts in fixed-bed and ebullating-bed residue hydroprocessing units

K. Al-Dalama*, A. Stanislaus

Petroleum Refining Department, Petroleum Research and Studies Center, Kuwait Institute for Scientific Research, P.O. Box 24885, Safat, Kuwait

Abstract

In residual oil upgrading by hydroprocessing, two types of reactor technologies namely, fixed-bed and ebullated-bed are commonly used. In this paper the deactivation behavior of catalysts in both types of units is compared based on the information obtained from the analysis of spent catalysts. In the fixed-bed unit, the concentration of vanadium deposits decreased from the entrance (first reactor) to the exit (last reactor), while, carbon content of the catalyst increased from the entrance to the exit. The loss of surface area for the catalysts in various reactors of the fixed-bed atmospheric residue desulfurization (ARDS) unit increased from the entrance to the exit. Distribution of the deposited vanadium with the catalyst pellet was also different in different reactors. Catalysts in the front-end reactors were deactivated mainly by metal deposition, while the back-end catalysts were primarily deactivated by coke deposition. The nature of the coke deposits on different catalysts was found to be significantly different by ^{13}C NMR, temperature programmed oxidation (TPO) and differential thermal analysis (TGA). Spent catalysts from the ebullated-bed reactor contained a mixture of highly fouled and partly fouled catalysts. The coke on the highly fouled spent catalyst particles was more aromatic and more condensed compared with that on the lightly fouled catalyst particles. Considerable changes in the physical dimensions of the catalyst pellets were noticed for the spent catalysts from the ebullating-bed reactor. In the ebullated-bed reactor, catalyst deactivation was caused not only by deposition of metals and carbon, but also by changes in the physical and mechanical properties of the catalyst under the dynamic conditions of the process.

Keywords: Fixed-bed; Ebullating-bed; Catalyst; Reactor

1. Introduction

Catalytic hydrotreating and hydroconversion processes are extensively used in the petroleum refining industry for the upgrading of heavy oils and residues. Two types of reactor technologies, namely, fixed-bed and ebullated-bed are commonly used in these processes [1–4]. In the fixed-bed process, pre-heated feed and hydrogen pass in the down-flow mode over a series of reactors packed with catalysts. In the ebullating-bed process, pre-heated feed and hydrogen enter the bottom of the reactor, and the catalyst bed is maintained in an ebullated (expanded) state by an upward flow of feed and the internal liquid recycles. In order to maintain a steady state activity, a provision is made for periodic catalyst addition and withdrawal [5,6].

The catalysts used in these processes deactivate rapidly, and many studies have been performed to understand the deactivation behavior of petroleum residue hydroprocessing catalysts [7–14]. The results of these earlier studies have revealed that the catalysts deactivate by the deposition of coke and metals. Blockage of pores caused by coke and metal deposits makes the active sites of the catalyst inaccessible to the reactants [15,16].

In the fixed-bed units, three stages of catalyst deactivation, namely, a rapid initial deactivation at the start of the run, a slower gradual deactivation at the middle of the run and a very rapid final deactivation at the end of the run have been observed [13,17–19]. It is a common practice to increase the reactor temperature gradually with time-on-stream to compensate for the loss of catalytic activity and to maintain constant hydrotreating performance in the fixed-bed residue hydroprocessing operations. In the ebullated-bed process, a portion of deactivated (equilibrium) catalyst is removed periodically from the bottom of the reactor and fresh catalyst is added to maintain the reactor performance at a steady level.

Deactivation of hydrotreating catalysts has been the subject of some investigation in this laboratory [20–27]. In a previous paper, we reported the relation between feed quality and coke formation in a three-stage fixed-bed atmospheric residue desulfurization process [26]. For the ebullated-bed residue hydrotreating process, information on catalyst deactivation is scarce. In the present paper the deactivation behavior of catalysts in the

* Corresponding author.
E-mail address: kdalama@yahoo.com (K. Al-Dalama).

1385-8947/$ – see front matter © 2006 Elsevier B.V. All rights reserved.
doi:10.1016/j.cej.2006.03.013

fixed-bed and ebullated-bed residue hydroprocessing operations is compared based on the information obtained through the analysis of spent catalysts from both types of units. This study is a continuation of our efforts to understand catalyst deactivation problem in residual oil hydroprocessing units.

2. Experimental

Samples of spent catalysts from fixed-bed and ebullated-bed residue hydroprocessing operations were obtained from Kuwait National Petroleum Company's Refineries. Schematic drawings of both types of reactor systems are shown in Fig. 1a and b. The ARDS unit has four reactors connected in series. The first one is a guard chamber loaded with 7% of the total catalyst. The catalysts used in all reactors were Co–Mo/Al_2O_3 type. The surface area, pore volume and metal (Co and Mo) content of the catalysts were, however, different. The front-end catalysts had wide pores (pore diameter in the range of 120–150 Å), whereas the back-end catalysts had narrow pores with pore diameter in the range of 80–100 Å. The other three reactors hold about 31% each of total catalyst. The feedstock processed in the ARDS unit was atmospheric residue of Kuwait export crude (S = 4.3 wt.%; V = 67 ppm; Ni = 20 ppm; N = 2500 ppm). Pre-heated feed and hydrogen enter the first reactor and pass through the catalyst beds in all four reactors in series maintained at the desired operating conditions.

The ebullated-bed unit consists of a single reactor loaded with the catalyst (Fig. 1b). The feed oil and hydrogen are heated to the required temperatures and then mixed in a specially designed mixture, before being introduced into the bottom of the reactor.

The catalyst bed is ebullated by the upward flow of the feed and the internal liquid recycle. A portion of the spent (equilibrium) catalyst is periodically withdrawn from the bottom and fresh catalyst is added to maintain steady state activity. A Ni–Mo/Al_2O_3 catalyst was used in the ebullated-bed reactor operation. The feedstock used in the ebullated-bed process was vacuum residue of Kuwait export crude diluted with about 10–15% recycled gasoil (S = 5.2 wt.%; metals [V + Ni] = 110 ppm; N = 4400 ppm).

In the case of the fixed-bed unit, the spent catalyst samples were collected from the bottom of each reactor. Since the catalysts were unloaded from the bottom of the reactors at the end of their life (350 days), the samples collected from the bottom will be more representative. For consistency, the spent catalysts for all experiments were collected from one batch. For the ebullated-bed reactor unit, spent catalyst sample was collected from the equilibrium catalyst withdrawn from the reactor. The spent catalysts were washed with toluene to remove contaminant oil and dried before subjecting them to further characterization. A sample splitter was used to obtain representative samples for chemical and physical analysis.

The carbon content of each sample was determined by elemental analysis using a CE instrument, model EA 1110. The concentrations of deposited metals (V and Ni) in the spent catalyst samples were determined using an inductively coupled argon plasma (ICP) spectroscopy (Jobin Yvon, model 24). An Autosorb adsorption unit, manufactured by Quantachrome Corporation, USA, was used for measuring of the surface area by BET method. Pore volumes of catalyst samples were determined by mercury intrusion using an Autoscan 60 porosimeter. A Quantachrome dual auto tap apparatus was used for bulk density measurements.

A scanning electron X-ray microprobe analyzer (Jeol SXA-8600) was used for measuring the concentration profiles of contaminated metals (V and Ni) across the catalyst pellet. A thermogravimetric analyzer (Shimadzu, model TGA-50) was used to measure the weight changes in catalyst samples as a function of temperature. A Shimadzu DTA-50 model differential thermal analyzer was used to measure the thermal characteristics of spent catalyst samples by measuring and recording both heating temperature and enthalpy.

Temperature programmed oxidation (TPO) analysis was done using a TGA-MS unit (TGA: Mettler Toledo model SDTA851; MS: Balzers model, Thermostat). About 20 mg of catalyst sample was heated in the presence of a gas mixture containing 15% O_2 in helium flowing at a rate of 60 ml/min, and the different gaseous products CO_2, SO_2 and NO_2 formed were monitored as a function of temperature using

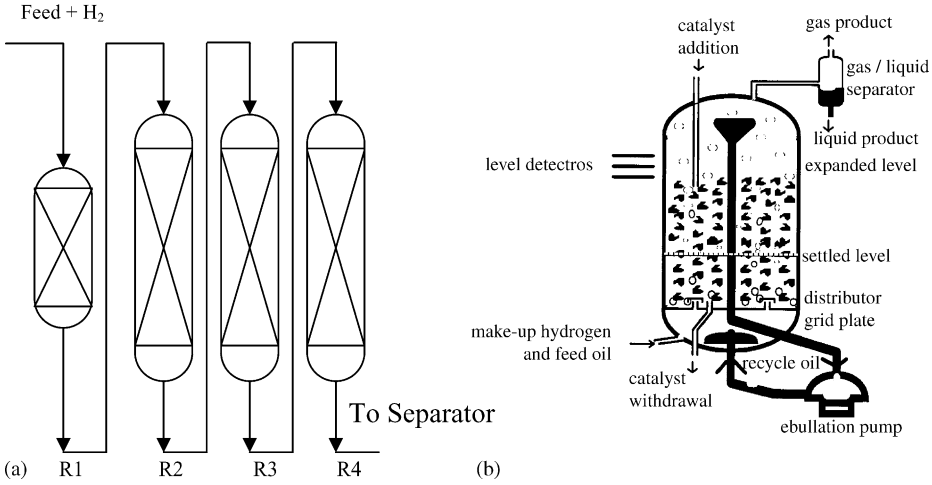

Fig. 1. (a) ARDS fixed-bed reactor unit. (b) Ebullated-bed reactor unit.

a mass spectrometer. A linear heating rate of 10 °C/min was used throughout the analysis. Solid-state ^{13}C NMR (Bruker Avance300 spectrometer) was used to quantify and characterize the carbon in different structural moieties present in the coke on catalysts. For more details see Hauser et al. [22].

For decoking of spent catalysts, a rotary furnace (Carbolite, model HTR 11/75) was used. A gas mixture containing 5% O_2 and 95% N_2 was used for coke combustion initially. The gas flow rate and furnace were controlled to keep the reactor temperature below 500 °C during the decoking operation. After burning a major part of the coke, the catalyst was heated in a current of air at 500 °C to burn traces of the remaining coke.

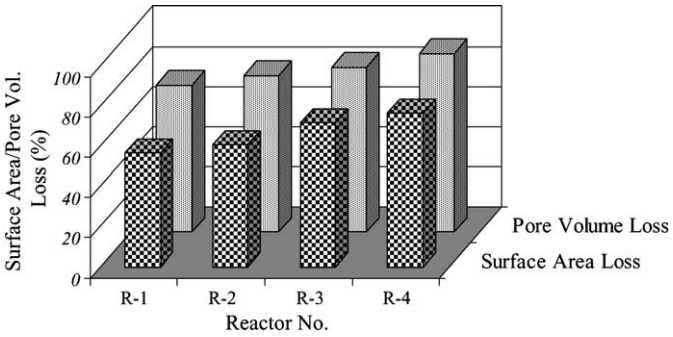

Fig. 3. Catalyst surface area and pore volume losses in different reactors.

3. Results and discussion

3.1. Catalyst deactivation in multiple reactor fixed-bed residue hydrotreators

Spent catalyst samples collected from different reactors of a four reactor industrial atmospheric residue desulfurization (ARDS) unit were first extracted with toluene in a soxhlet apparatus to remove the oil residues and then characterized by chemical analysis and other techniques. The amounts of carbon and metals (V and Ni) deposited on the catalysts in different reactors are presented in Fig. 2. The results show the following trends.

In a series of four reactors in the ARDS unit, the concentration of vanadium and nickel deposited on the catalyst decreases from the first reactor to the last reactor. Carbon deposition on the catalyst shows the opposite trend. It increases from the first reactor to the last reactor. Surface area and pore volume losses are highest for the catalyst in the last reactor and lowest for the catalyst in the first reactor (Fig. 3). On decoking, the surface area recovery is considerably higher for the catalysts from the back-end reactors compared with the front-end reactors. The pore volume improvement after decoking is also substantially higher for the back-end reactors (Fig. 4). These results can be explained as follows.

In a four-reactor ARDS unit, the metals containing feed enters the first reactor and passes through the catalyst bed in the 1st, 2nd, 3rd and 4th reactors in series, where it undergoes hydroprocessing in sequence and the end products leave from the last reactor. In the first reactor, where the feed comes into contact with the catalyst, hydrodemetallization (HDM) reactions begin to occur and the metals removed from the feed start depositing on the catalyst surface. As more and more feed is processed, more and more metals continue to deposit on the catalyst surface. Accumulation of the metals causes deactivation of the catalyst in the first reactor. As a result, metals and the other impurities present in the feed come into contact with the catalyst in the next reactor in the series (reactor 2) and the metals start depositing on the catalyst in this reactor. With longer processing time, the activity of the catalyst in reactor 2 declines due to the accumulation of metals, and the contaminant metals find their way to the other reactors in the series. The capacity for metals uptake is usually different for different catalysts and decreases from reactors 1 to 4 [28,29]. In agreement with this, the contaminant metal (e.g. V) content is the highest in the first reactor and the lowest in the last reactor.

Unlike the metal deposits, the amount of carbon deposited on the catalyst increases progressively from reactors 1 to 4 in the series. In other words, the minimum deposition of carbon occurs in the first reactor and increases towards the last reactor. This trend in coke deposition may be attributed to a combination of factors, such as changes in the quality of the feed entering different reactors as well as to variations in hydrogen partial pressure. In the first reactor, the atmospheric residue feed is partially demetallized and desulfurized over a HDM catalyst. This partially hydrotreated product from the first reactor may contain

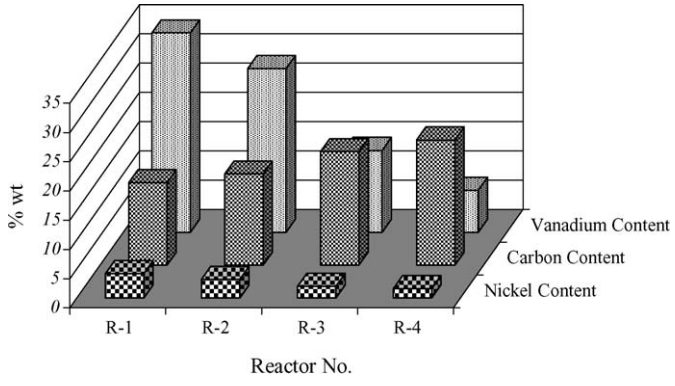

Fig. 2. Amount of carbon, nickel and vanadium deposits on spent catalysts in different reactors.

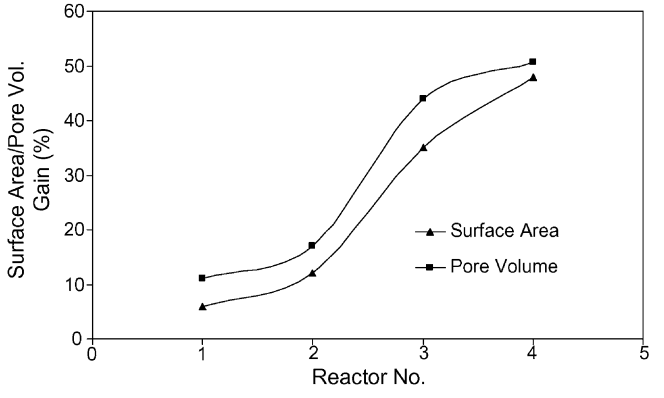

Fig. 4. Surface area and pore volume increase after decoking for catalysts in different reactors.

reaction intermediates such as unstable radicals and low reactive polynuclear aromatic hydrocarbons present in the original feed as well as highly condensed asphaltenes that have a high propensity for coke formation. With increasing processing time, the concentrations of these coke precursors in the products from the front-end reactors increase progressively and pass on to the other reactors in sequence and can, thus, enhance coke formation in the back-end reactors. This process is further accelerated by a progressive decrease in the hydrogen partial pressure from the first to the last reactor due to the presence of H_2S and light hydrocarbons in the hydrogen stream.

The surface area and pore volume data in Figs. 3 and 4 indicate that for the front-end catalysts that have accumulated more metal deposits than coke, the surface area and pore volume recovery after coke removal is very low implying that both the surface area and pore volume losses in these catalysts are caused mainly by metal deposits. Coke plays only a minor role in the deactivation of the front-end catalysts by surface area and pore volume loss. In the back-end catalysts the gain in surface area and pore volume after coke removal is remarkably high. The results suggest that coke deposition is the dominant cause for pore volume loss in the last reactor, whereas metal deposition is primarily responsible for porosity loss in the first reactor.

In addition to the chemical analysis and physical properties tests, some special tests such as temperature-programmed oxidation (TPO), differential thermal analysis (DTA), ^{13}C NMR and electron microprobe analysis were used to characterize the spent catalyst samples from different reactors.

3.2. TPO

The spent catalyst samples collected from different reactors were subjected to TPO with a gas mixture containing 5% O_2 in helium. A linear heating rate of 10 °C/min was used throughout, and the different gaseous products formed during coke oxidation were monitored as a function of temperature using a mass spectrometer. The main purpose of the study was to obtain information on the nature of the coke deposits on the catalysts in different reactors and their reactivities.

During the TPO of spent catalyst samples, oxides of C, S and N were formed indicating the presence of C, N, and S in the spent catalysts. The peak shapes and peak temperatures of the gases evolved during the TPO runs differed considerably for the spent catalysts from different reactors. The TPO profiles and peak temperatures observed for the major products, i.e. CO_2, SO_2 and NO_2, formed during the TPO of spent catalysts from all four reactors are compared in Figs. 5–7, respectively. CO_2 formation during the TPO of the spent catalyst of reactors 1 and 2 shows a major peak at 380 °C with an unresolved second peak appearing as a shoulder at 430 °C (Fig. 5). In the case of the spent catalyst from the back-end reactors (3 and 4), a single broad peak with a maximum around 420–430 °C is seen for CO_2 emission. The temperatures at which coke oxidation starts and ends increase progressively from reactors 1 to 4. Thus, for example, coke oxidation for spent catalyst from the front-end reactor 1 and 2 starts at a temperature around 200 °C and ends at 450 °C, whereas in the case of spent catalyst from reactor 4,

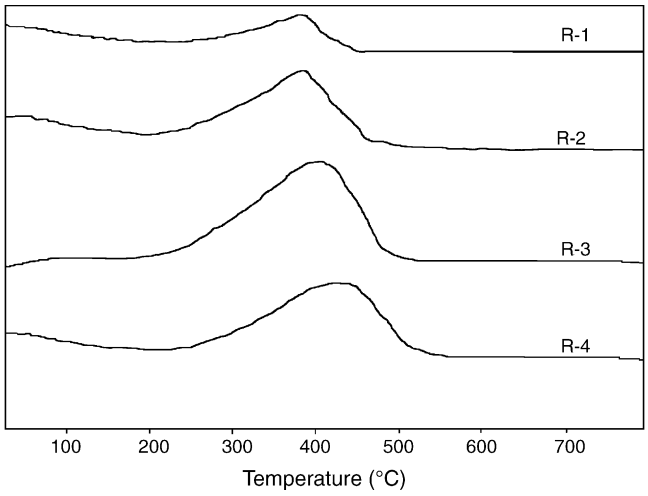

Fig. 5. CO_2 profiles for TPO of spent catalyst samples from different reactors.

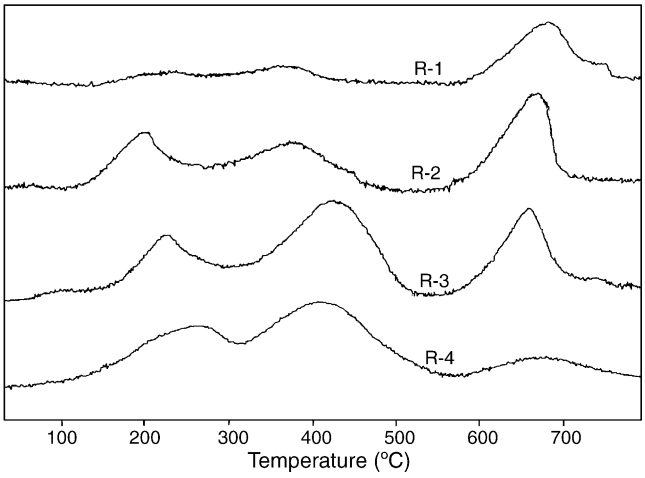

Fig. 6. SO_2 profiles for TPO of spent catalyst samples from different reactors.

coke oxidation starts at 250 °C and is complete at 550 °C. The temperature at which CO_2 peak maximum occurs increases from 380 to 440 °C as we move from reactor 1 to reactor 4. The exact reasons for this difference in the coke combustion temperature range are not clear. Analytical data indicate that the spent catalyst

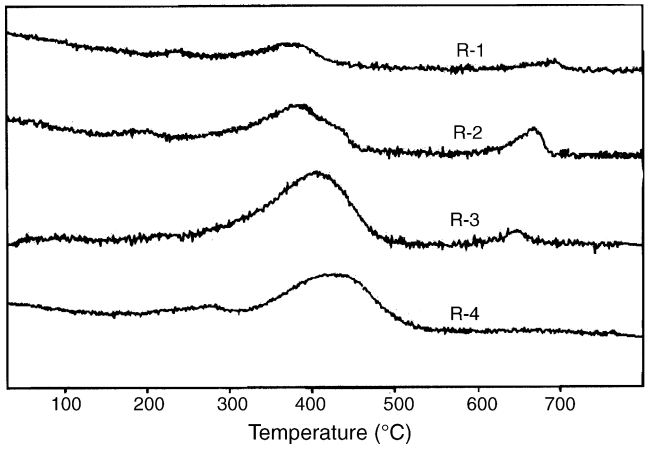

Fig. 7. NO_2 profiles for TPO of spent catalyst samples from different reactors.

from different reactors have different vanadium contents. The vanadium contents of spent catalysts decrease from reactor 1 to reactor 4. Spent catalysts from reactor 1, which contain a larger concentration of vanadium, exhibit a lower temperature range for coke oxidation. It appears that the V present in the spent catalyst enhances the oxidation of coke. Vanadium-catalyzed oxidation of coke has been reported earlier by Massoth [30] and Zeuthen et al. [31].

The TPO profiles for SO_2 show three peaks (Fig. 6). The oxidation of sulfur occurs even before the coke oxidation and formation of CO_2 starts. The absence of a CO_2 peak coinciding with the first (240 °C) and the third (690 °C) SO_2 peaks suggests that the form of sulfur, which oxidizes at these temperatures, is not associated with coke. From the TPO of fresh sulfided catalyst, it has been found that the oxidation of Ni/Mo sulfides to SO_2 occurs between 200 and 250 °C. Therefore, as suggested by previous workers [32–37] the first broad low-temperature SO_2 peak can be attributed to the oxidation of metal sulfides present in the catalyst. The second SO_2 peak appears exactly in the temperature region, where major part carbon combustion to CO_2 takes place indicating that the organic sulfur present in the coke is oxidized together with carbon in this temperature region. The spent catalysts from all reactors also exhibit high-temperature SO_2 peaks occurring between 600 and 700 °C. No CO_2 peak coincides with this high-temperature SO_2 peak. This high-temperature SO_2 peak could be attributed to the decomposition of metal sulfates to SO_2. Under oxidizing conditions at temperatures around 500 °C, metal sulfates such as $Al_2(SO_4)_3$ could be formed by reaction of sulfur oxides with Al_2O_3, which may undergo thermal decomposition to metal oxide and SO_2 at higher temperatures [38]. As in the case of CO_2 formation, the positions of first two peaks are shifted to lower temperatures in moving from the back-end to front-end reactors due to the accelerating influence of vanadium.

The NO_2 profiles are also different for different catalysts (Fig. 7). In the case of the spent catalyst from reactors 1 and 2, three peaks coinciding with the three SO_2 peak temperatures are noticed, which indicate that three types of nitrogen species are present in these catalysts. One type of nitrogen is oxidized with the formation of a peak at temperatures around 240 °C. Since this peak appears before the occurrence of a CO_2 peak and coincides with first SO_2 oxidation peak, it is reasonable to suggest that this type of nitrogen species is associated with the active sulfide (Ni–Mo–S) phase. The basic nitrogen compounds present in the residual oil could be strongly adsorbed on the coordinatively unsaturated sites of active metal sulfide phase of the catalyst, and could be oxidized with the S in the metal sulfides to form nitrogen oxides together with SO_2.

The second type of nitrogen is associated with coke and oxidizes together with carbon forming a peak at a temperature of around 380 °C, coinciding with the prominent CO_2 peak. The third nitrogen species is oxidized at very high temperatures close to 700 °C. The peak for this nitrogen species coincides with the high temperature SO_2 peak formed by the decomposition of metal sulfates. It is likely that a part of the nitrogen is associated with the metal sulfates or present as metal nitrates which decompose in this temperature region. But more work is needed to identify the species involved.

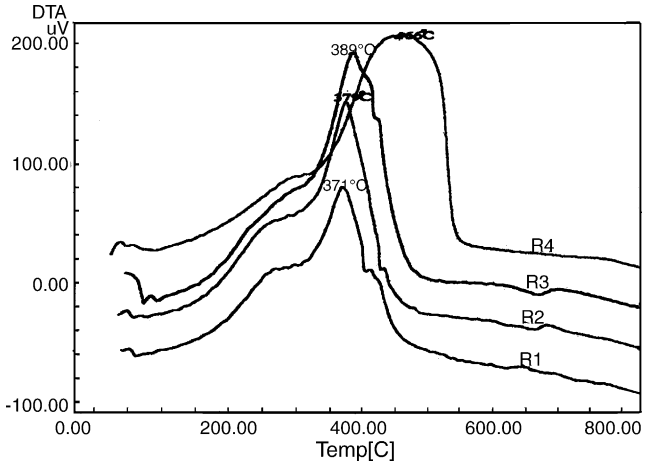

Fig. 8. Differential thermal analysis curves for spent ARDS catalysts from the four reactors.

3.3. DTA

DTA profiles of the spent catalyst samples from different reactors are compared in Fig. 8. The results indicate the following: the DTA profile of each catalyst has three exothermal peaks. The temperatures at which the exothermal peaks appear are slightly different for different catalysts. The first exothermal peak appears in the temperature region of 240–270 °C for the 1st and 2nd reactor catalysts, but they are shifted to a slightly higher temperature (i.e. 300 °C) for the 3rd and 4th reactor spent catalyst. The second exothermal peaks are relatively large for all catalysts and the peak temperatures show a substantial increase from the 1st to the last reactor. The third exothermal peak appears as an unresolved protrusion after the 2nd peak.

The oxidative reactions of carbon, sulfur, and nitrogen that occur during coke combustion are exothermic and yield high heats of reaction that are shown as exothermic peaks in the DTA plots [32]. The first exothermal peak appears in the temperature region of 240–270 °C where the metal sulfide oxidation occurs. Therefore, the first broad exothermal peak in the DTA plots in Fig. 8 can be assigned to metal sulfides oxidation.

The temperature at which the second peak appears (370–450 °C) matches the coke oxidation temperature region observed in the temperature-programmed oxidation (TPO) of coke on spent catalysis. The progressive shift in the coke oxidation peak temperature to a higher region with decreasing vanadium content of the catalyst as one moves from the first to the last reactor is consistent with the TPO results and confirm the role played by vanadium in coke oxidation.

Fig. 9 shows the weight loss curves as a function of temperature obtained by thermogravimetric analysis (TGA) of spent catalyst samples from the four reactors. Three different zones of weight loss are noticed in the curves. These three zones correspond exactly to the three exothermal peaks observed in the DTA curves and, hence, provide additional evidence for the

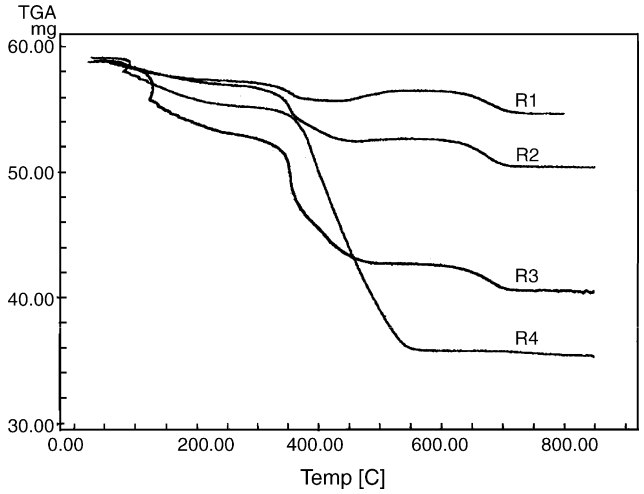

Fig. 9. Thermal gravimetric analysis curves for spent catalysts from four reactors.

conclusion reached in the DTA and TPO studies concerning coke and metal sulfide oxidation.

3.4. Coke characterization by ^{13}C NMR spectroscopy

Spent catalyst samples collected from different reactors were further characterized by ^{13}C NMR analysis to obtain information about the nature of the coke deposits on the catalyst.

The aromaticity of the deposited coke and different types of aromatic carbon in the coke, such as tertiary, quaternary, alkyled substituted and carbon in bridge head positions of fused aromatic rings were quantitatively estimated from the ^{13}C NMR signals assigned to these structural groups. The procedures used for the NMR technique have been described in a previous paper [22]. The results are presented in Table 1.

The results show that the coke deposits in the back-end reactor catalysts are more aromatic and contained less amount of alkyl groups than that of the front-end catalysts. The aromatic carbons in bridge-head portions, which indicate the degree of condensation of coke structure, are not appreciably different in different spent catalysts.

3.5. Distribution of deposited metals

Distribution profiles of the deposited metals (V and Ni) within the spent catalyst pellets picked from different reactors and measured by electron microprobe analysis, show that vanadium distribution across the pellet cross-section is higher and more uniform in reactor 1 spent catalyst than the others (Fig. 10). Vanadium concentration decreases towards the center of the pellet and that near the outer edge sharply increases in moving from the first to the last reactor in the series.

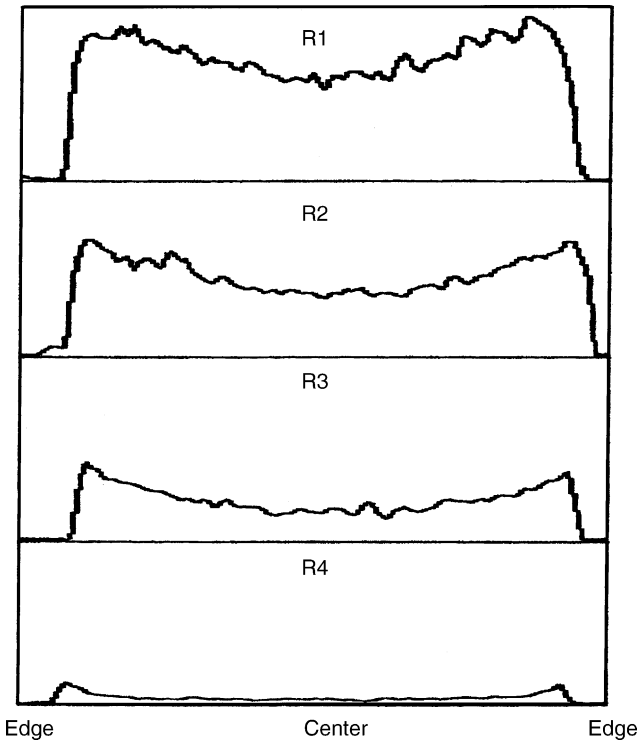

Fig. 10. Distribution profiles of vanadium within the decoked catalyst pellets sampled from different reactors.

The variation in the distribution profiles of vanadium can be attributed to the differences in the pore size and composition of the different types of catalysts in different reactors since these parameters determine the diffusion rate and the chemical reaction rate of the metal-containing molecules [39]. The catalyst in the first reactor has larger pores and low intrinsic activity. The ratio of diffusion rate to chemical reaction rate is high in such catalysts. Consequently, the metal-bearing molecules diffuse deeper into the pores and the metal deposits are homogeneously distributed. The catalysts in the back-end reactors have narrow pores and high intrinsic activity. In narrow pore catalysts, the diffusion rates are low, and due to the high intrinsic activity, the ratio of chemical reaction to diffusion rate will be high. Hence, the metal-containing molecules react as soon as they enter the pores, depositing more metals near the pore mouths. Non-uniform vanadium distributions

Table 1
Aliphatic, total aromatic and aromatic carbon distribution in the spent ARDS catalysts from different reactors

Sample	Aliphatic carbon	Total aromatics	Tertiary	Quarternary	Distribution of aromatic carbon			
					Alkyl substituted	3-Ring junction	2-Ring junction	Rest
R1	24	76	5	71	28	5	21	17
R2	18	82	6	76	26	5	25	20
R3	16	84	25	29	14	4	21	20
R4	11	89	35	54	14	5	24	11

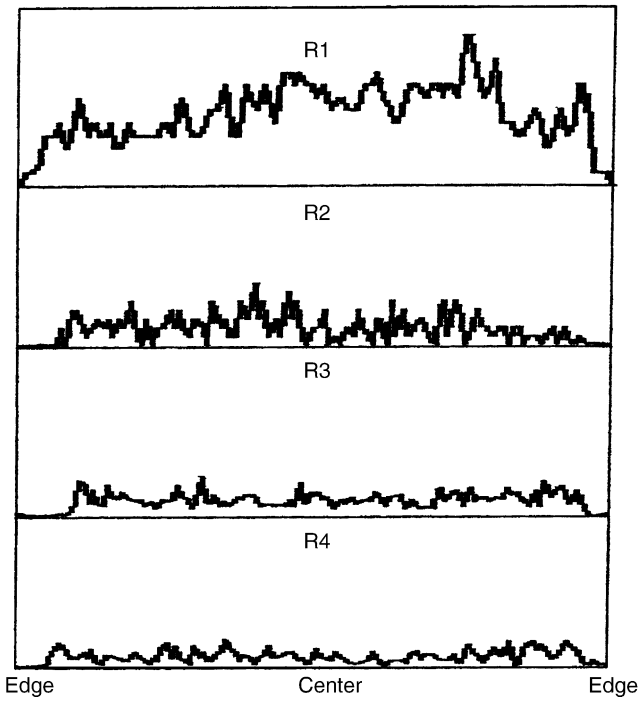

Fig. 11. Distribution profiles of nickel within the spent catalyst pellets samples from different reactors.

with maximum concentrations at the edges, observed for the spent catalysts in reactor 3 and 4, are in agreement with this argument.

Nickel distribution within the pellet was found to be more uniform than vanadium (Fig. 11). The differences in depositional patterns between nickel and vanadium can be explained in terms of the differences in the reactivities and diffusivities of the molecular species containing these metals. Studies have shown that nickel-containing molecules in residual oil diffuse more easily into the catalyst pores than the vanadium-containing species [39]. It is reported that the effective diffusivity for nickel is almost twice that of vanadium. As for the reactivities of two metals, hydrometallization studies with residues as well as with model compounds have shown that vanadium removal rates exceed those of nickel. It has been suggested that the vanadium compounds are more reactive because the vanadium is coordinated with the protruding oxygen atom, and this makes them more subject to attack [39]. The lower reactivity of nickel together with its higher diffusion rates, thus, appears to be responsible for its deeper penetration into the catalyst pellet. In consequence, nickel is more uniformly deposited throughout the catalyst pellet even in narrow pore catalysts compared with that of vanadium.

3.6. Catalyst deactivation in ebullated-bed residue hydroprocessing units

In the ebullated-bed process, the catalyst bed is expanded by the upward flow of the feed recycle oil and hydrogen from the bottom of the reactor. The feedstock, hydrogen and extrudate catalyst particles are brought together in constant motion.

Table 2
Characteristics of heavy and light portions of spent NiMo catalysts from an industrial ebullated-bed reactor unit

Catalyst property	Spent mix	Fouled light	Heavily fouled
Chemical properties			
V (wt.%)	10.58	4.37	13.83
C (wt.%)	16.20	15.80	16.30
Ni (wt.%)	4.03	3.48	5.21
Physical properties			
Surface area (m^2/g)	68	122	55
Bulk density (g/m)	1.09	0.97	1.21
Side crushing strength (lb/mm)	1.80	2.10	1.78
Pore volume (ml/g)	0.17	0.21	0.11
Particle length distribution (wt.%)			
<1.5 mm	25.2	14.4	40.0
1.5–3.0 mm	42.3	23.5	37.0
3.0–6.0 mm	32.5	61.3	23.0
>6.0 mm	0.0	0.8	0.0

Spent catalysts from the ebullated-bed reactor contained a mixture of highly fouled and partly fouled catalysts. They were separated by jigging technique using a mineral jig (Model IM, Denver Equipment, England), and then characterized. The characteristics of the heavy and light portions of the spent catalysts are presented in Table 2. It is seen that the heavily fouled catalyst has substantially more vanadium (14 wt.%) than the lightly fouled ones (V = 4.4 wt.%). The carbon content does not differ appreciably between the two types of spent catalyst particles and remains constant at around 16 wt.%. The surface area and pore volume of the lightly fouled spent catalyst particles are substantially higher than that of the heavily fouled catalyst particles. Since fresh catalyst is added and spent catalyst is withdrawn periodically in ebullated-bed reactors, and since the catalyst particles are in continuous motion, it is likely that a portion of the catalyst, which is not fully deactivated by metal deposition is also withdrawn. The percentage of the vanadium in the spent catalyst particles reflect the age of the catalyst in the reactor, and indicate that the catalyst with high-vanadium content (heavily fouled particle) has been in the reactor for a longer period of time than the low-vanadium content particle. Deposition of metals on the catalyst increases its bulk density. The heavily fouled spent catalyst particles with higher vanadium content have a higher bulk density than the lightly fouled catalyst.

Considerable changes in the physical dimensions of the catalyst pellets are also noticed for the spent catalyst from the ebullating-bed reactor (Table 2). Particle length distribution is significantly altered with a remarkable increase in the percentage of smaller particles. The fresh catalysts usually have around 1% of the small particle with length less than 1.5 mm, but in the spent catalyst about 25% of the particles have length less than 1.5 mm. The percentage particles in the larger length range (3–6 mm) is reduced from 70% in the fresh catalysts to around 32% in the spent catalysts. The particle length reduction is considerably larger in the case of the heavily fouled spent catalysts. Forty percent of the particles in the heavily fouled catalyst portion have length less than 1.5 mm compared with 14.4% in the

lightly fouled catalysts. About 61% of the lightly fouled catalyst particles have larger length in the range of 3–6 mm whereas only 23% of the heavily fouled spent catalysts have length in this range.

The physical dimensions of the catalyst (particle length, diameter, shape, etc.) play an important role in the ebullation behavior of the catalyst bed. If the particle dimensions are very small, a large proportion of the catalyst will tend to float over the top of the bed. As a result, the bed uniformity will be affected and catalyst carry-over is possible. On the other hand, if the particle size is too large, the bed expansion will be low. This is undesirable since low bed expansion will affect the mixing pattern and reduce the catalyst contact with oil and hydrogen. The bulk density of the catalyst also has a significant effect on the bed expansion. A higher bulk density will require more ebullating fluid flow to achieve the required bed expansion. In contrast, if the particles are light and have low density, the catalyst will require low fluid flow that may affect the reactor's mass and heat balance.

The length distribution and bulk density of fresh catalysts used in the ebullated-bed hydroprocessing units are usually made to meet the specifications for the designed expansion of catalyst-bed in the reactor. The results of the present studies clearly show that in the ebullated-bed reactor, catalyst deactivation and malfunctioning is caused not only by deposition of metals and carbon, but also by changes in the physical and mechanical properties of the catalyst under the dynamic conditions of the process.

The coke deposit on the two types of spent catalysts picked from the ebullated-bed hydroprocessing unit was further characterized by TPO and NMR. The TPO profiles of the various gases (CO_2, SO, SO_2, NO and NO_2) produced during TPO of the heavily fouled and lightly fouled catalyst samples are presented in Figs. 12 and 13. In both samples carbon combustion starts at a temperature around 220 °C and ends at temperature around 500 °C. The CO_2 produced during the TPO shows two broad overlapping peaks in both cases indicating the presence of two types of coke. Several authors have reported the presence of two kinds of coke, a reactive soft coke, which can be removed more easily at low temperatures, and a refractory hard coke,

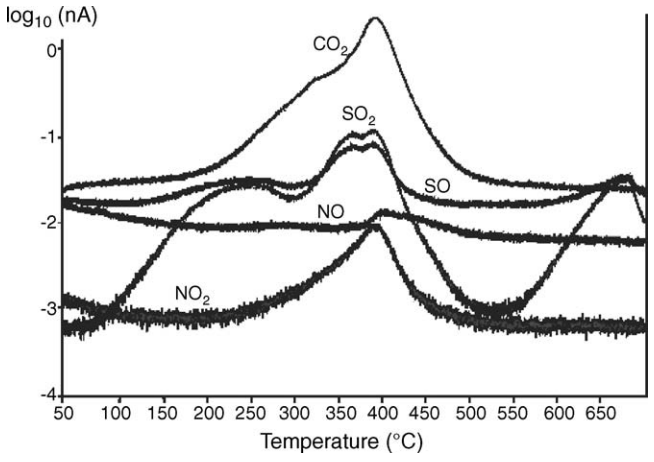

Fig. 12. TPO profiles of various gases produced from heavily fouled spent catalyst sample.

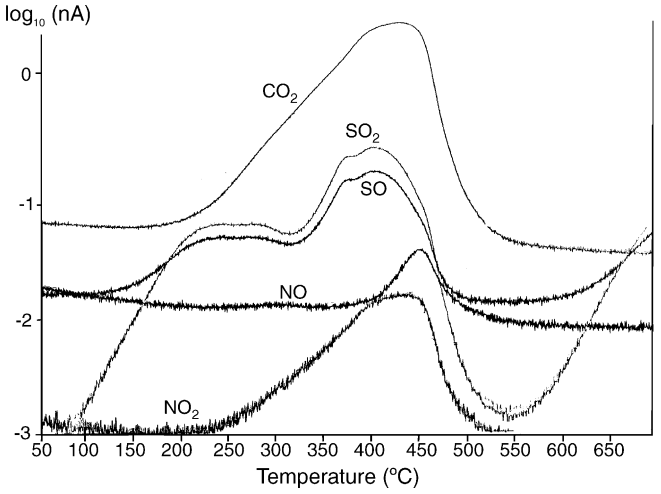

Fig. 13. TPO profiles of various gases produced from lightly fouled spent catalyst sample.

which requires higher temperatures for combustion [31,35,37]. The CO_2 peak positions are, however, slightly different for the two samples. In the sample with high vanadium content (heavily fouled), the CO_2 peak maximum occurs at a lower temperature compared with that for the lightly fouled catalyst sample. This is consistent with the results reported earlier for the fixed-bed catalysts.

Sulfur oxides (SO and SO_2) formation from both samples during TPO occurs at three temperature regions with three peaks. The TPO profiles of SO and SO_2 are similar in both types of spent catalyst samples. The first peak appearance in the temperature region of 200–250 °C could be assigned to SO_2 formation from the oxidation of metal sulfides as discussed earlier under the TPO results of fixed-bed spent catalysts. In temperature region of 325–450 °C, SO and SO_2 profiles exhibit two overlapping peaks with maximum at temperatures 350 and 390 °C. Since these peaks coincide exactly with the CO_2 peaks, it is possible to suggest that the sulfur oxides formed in this temperature region originate from the oxidation of sulfur associated with coke in the catalyst.

The third SO_2 peak which occurs at a higher temperature of 650 °C is similar to that observed in the case of fixed-bed spent catalysts and could be assigned to the decomposition of metal sulfates as previously discussed. The last two SO_2 peaks formed by the oxidation of S in the coke and by the decomposition of metal sulfates, respectively, are shifted slightly to a lower temperature region in the highly fouled catalyst and confirm that the vanadium present in the spent catalysts enhances S oxidation and decomposition of sulfates to sulfur oxides the same way as coke oxidation to CO_2.

The oxidation of nitrogen present in both types of spent catalysts to nitrogen oxides (NO and NO_2) takes place in the same region where carbon combustion occurs which indicates that the nitrogen is associated with coke. The starting of NO formation and its peak maximum, however, occur at a slightly higher temperature than that for NO_2 in both types of catalysts. A part of the nitrogen, which is preferentially adsorbed on the acid sites, may remain beneath the coke layer. The asphaltenes and polynuclear

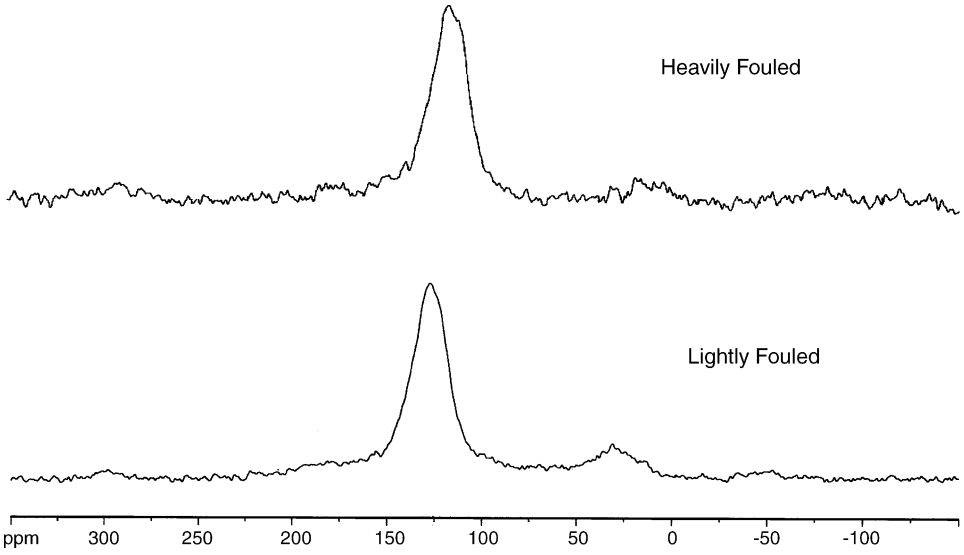

Fig. 14. ^{13}C NMR spectra of coke deposits on lightly fouled and heavily fouled catalysts.

aromatics compounds present in the residual oil feed contain heterocyclic nitrogen compounds that are more susceptible to coke formation due to their strong interaction with the acid sites of the catalyst surface [40,41]. The oxidation of this nitrogen is likely to start after a large part of the coke is removed by combustion. Zeuthen et al. [42] have made similar observation during the TPO of nitrogen aged hydroprocessing catalysts. The peak positions of both nitrogen oxides (NO and NO_2) in the two types of catalysts are slightly different. In the case of the highly fouled spent catalyst, the peak maximum for both oxides occur at a lower temperature than that of the low-vanadium containing lightly fouled catalyst in much the same way as the CO_2 and SO_2 formation peaks, and indicates the accelerative influence of vanadium on the oxidation of nitrogen present in the coke during coke combustion.

^{13}C NMR spectra of coke deposits on the lightly fouled and heavily fouled catalysts are compared in Fig. 14. The regions from 0 to 70 ppm and 90–190 ppm are attributed to the aliphatic carbon and total aromatic carbon, respectively. The distribution of different types of aromatic carbons in both types of catalysts estimated from the NMR signals is compared in Table 3.

It is seen that the coke on the heavily fouled spent catalyst particles is more aromatic and more condensed with less number of alkyl substituents compared with that on the lightly fouled catalyst particles. Since the highly fouled spent catalyst has been in the reactor for a longer period of operation, it is likely that the coke deposits have undergone further reactions such as dealkylation, dehydrogenation and condensation under the high temperature conditions resulting in a more aromatic coke with a lower number of alkyl substituents.

Table 3
NMR data for coke deposits formed on lightly fouled and heavily fouled spent catalysts

NMR data	Lightly fouled spent catalyst	Heavily fouled spent catalyst
Total aromatic carbon, Car (wt.%)	87	94
Tertiary aromatic carbon, Car, t (wt.%)	52	47
Quaternary aromatic carbon, Car, q (wt.%)	35	47
Triple bridged aromatic carbon, Car, b3	4	10
Double bridged aromatic carbon, Car, b2	15	22
Alkyl substituted aromatic carbon, Car, R	16	13
Aromaticity (fa)	0.87	0.94
Degree of condensation (γ)	0.22	0.35
Degree of substitution (σ)	0.24	0.21

4. Summary and conclusions

In the present work, the deactivation behavior of catalysts in industrial fixed-bed and ebullated-bed residue hydroprocessing units was investigated through detailed characterization of the spent catalysts collected from these units. Spent catalyst samples were obtained from Kuwait refineries. They were soxhlet extracted with toluene to remove the oil residues and then analyzed to determine the amount of coke and metal (V and Ni) deposits. The catalysts were also characterized by surface area and pore volume measurements, TPO analysis, DTA and TGA along with ^{13}C NMR and electron microprobe analysis. The important results and conclusions of the studies are summarized below.

4.1. Fixed-bed unit

Spent catalysts from the four-reactor fixed-bed unit, contained coke and metal (V and Ni) deposits, but the amount of coke and metals were different in different reactors. The concentration of metals decreased from the first reactor to the last reactor, while carbon content of the catalyst showed the opposite trend. Surface area and pore volume losses were higher for the catalysts in the back-end reactors. For the front-end catalysts, that had accumulated more metals than coke, the surface area and pore volume recovery after decoking was very low implying that both surface area and pore volume losses in the catalyst were caused mainly by metal deposits. In the back-end catalysts, the gain in surface area and pore volume after coke removal was

remarkably high indicating that coke deposition was the dominant cause of the deactivation of these catalysts.

TPO, DTA and ^{13}C NMR analysis showed significant differences in the nature of the coke deposits on different catalysts. Heteroatoms such as nitrogen and sulfur were present in the coke and they were oxidized to NO_2 and SO_2 during TPO. The peak positions of CO_2, SO_2 and NO_2 gases formed during TPO were shifted to lower temperatures with increasing vanadium content the spent catalysts due to the accelerating influence of vanadium on the oxidation of coke and the S and N species in the coke. ^{13}C NMR results showed that the coke deposits in the back-end reactor catalysts were more aromatic and contained less amount of alkyl groups than that of the front-end catalysts. The degree of condensation of coke structure, were not appreciably different in different spent catalysts.

Distribution profiles of the deposited metals (V and Ni) within the spent catalyst pellets picked from different reactors and measured by electron microprobe analysis, showed that vanadium distribution across the pellet cross-section was higher and more uniform in reactor 1 spent catalyst than the others. Vanadium concentration decreased towards the center of the pellet and that near the outer edge sharply increased in moving from the first to the last reactor in the series. Nickel distribution within the pellet was found to be more uniform than vanadium in the spent catalyst samples from all four reactors.

4.2. Ebullated-bed unit

Spent catalysts from the ebullated-bed reactor contained a mixture of highly fouled and partly fouled catalysts. The heavily fouled catalyst contained a substantially more amount of vanadium (14 wt.%) than the lightly fouled ones (V = 4.4 wt.%). The carbon content did not differ appreciably between the two types of spent catalyst particles. However, the aromaticity and TPO profiles of coke on the two types of catalysts were significantly different. The surface area and pore volume of the lightly fouled spent catalyst particles were substantially higher than those of the heavily fouled catalysts. Since fresh catalyst is added and spent catalyst is withdrawn periodically in ebullated-bed reactors, and since the catalyst particles are in continuous motion, it is likely that a portion of the catalyst, which is not fully deactivated by metal or coke deposition is also withdrawn. Considerable changes in the physical dimensions of the catalyst pellets were also noticed for the spent catalyst from the ebullating-bed reactor. Particle length distribution was significantly altered with a remarkable increase in the percentage of smaller particles having length less than 2 mm; this could affect the bed uniformity and mixing pattern in the reactor. In the ebullated-bed reactor, catalyst deactivation was caused not only by deposition of metals and carbon, but also by changes in the physical and mechanical properties of the catalyst under the dynamic conditions of the process.

References

[1] J.F. Le Page, Resid and Heavy Oil Process, Editions Technip, Paris, 1992.
[2] M.R. Gray, Upgrading Petroleum Residues and Heavy Oils, Marcel Dekker, New York, 1994.
[3] Furimsky, Appl. Catal. A: Gen. 171 (1998) 177–206.
[4] S. Kressmann, F. Movel, V. Harle, S. Kasztellan, Catal. Today 43 (1998) 203–215.
[5] R.M. Eccles, Fuel Process. Technol. 35 (1993) 21–38.
[6] E.K.T. Kam, M.M. Mishan, H. Dashti, Stud. Surf. Sci. Catal. 100 (1996) 283–292.
[7] J. Bartholdy, B.H. Cooper, Metal and coke deactivation of resid hydroprocessing catalysts, in: ACS Symposium on Resid Upgrading, Denver, CO, USA, 1993.
[8] K. Edi, T. Takahashi, T.J. Kai, Jpn. Petrol. Inst. 46 (2003) 45–52.
[9] M. Absi-Halabi, A. Stanislaus, D.L. Trimm, Appl. Catal. 72 (1991) 193–215.
[10] C.H. Bartholomew, Catalyst deactivation in hydrotreating of residues, in: M.O. Balla, S.S. Shih (Eds.), Catalytic Hydroprocessing of Petroleum and Distillates, Marcel Dekker, New York, 1994, p. 32.
[11] G. Gualda, Kasztelan, Stud. Surf. Sci. Catal. 88 (1994) 145–154.
[12] M.A. Callejas, M.T. Martinez, J.L.G. Fierro, C. Rial, J.M.J. Mateos, F.G.G. Garcia, Appl. Catal. A: Gen. 220 (2001) 93–104.
[13] P.W. Tamm, H.F. Harnsberger, A.G. Bridge, Ind. Eng. Chem. Process Des. Dev. 20 (1981) 262–273.
[14] E. Furimsky, F.E. Massoth, Catal. Today 52 (1999) 381–495.
[15] F.M. Dautzenberg, J. Van Klinken, K.M.A. Pronk, S.T. Sie, J.B. Wiffels, ACS Symp. Ser. 65 (1978) 254–265.
[16] S.T. Sie, in: B. Delmon, G.F. Froment (Eds.), Catalyst Deactivation by Poising and Pore Plugging to Petroleum Processing in Catalyst Deactivation, Amsterdam, Elsevier, 1980, pp. 545–569.
[17] P. Hannerup, A.C. Jacobson, ACS Petrol. Div. Prepr. 28 (1983) 576–583.
[18] T.M. Oelderik, S.T. Sie, D. Bode, Appl. Catal. 47 (1990) 1–24.
[19] E.K.T. Kam, M. Al-Shimali, M. Juraidan, H. Qabazard, Energy Fuels 19 (2005) 753–764.
[20] M. Absi-Halabi, A. Stanislaus, ACS Symp. Ser. 234 (1996) 229–237.
[21] A. Marafi, S. Fukase, M. Al-Marri, A. Stanislaus, Energy Fuels 17 (2003) 661–668.
[22] A. Hauser, A. Marafi, A. Stanislaus, A. Al-Adwani, Fuel 84 (2005) 259–269.
[23] A. Marafi, A. Stanislaus, Appl. Catal. 159 (1997) 259–267.
[24] K. Matsushita, A. Hauser, A. Marafi, A. Stanislaus, Fuel 83 (2004) 1031–1038.
[25] K. Matsushita, A. Hauser, A. Marafi, A. Stanislaus, Fuel 83 (2004) 1669–1674.
[26] A. Hauser, A. Marafi, A. Stanislaus, A. Al-Adwani, Energy Fuels 19 (2005) 544–553.
[27] M. Absi-Halabi, A. Stanislaus, T.L. Mughni, S. Khan, A. Qamra, Fuel 74 (1995) 1211–1215.
[28] C.T. Adams, A.A. Del Peggio, H. Schaper, W.H.J. Stork, W.K. Shiflett, Hydrocarb. Process. (1989) 57–63.
[29] J.M. Oelderik, S.T. Sie, D. Bode, Appl. Catal. 47 (1989) 1–24.
[30] F.E. Massoth, Fuel Process. Technol. 4 (1981) 63–71.
[31] P. Zeuthen, J. Bartholdy, F.E. Massoth, Appl. Catal. A: Gen. 129 (1995) 43–55.
[32] P. Dufresne, ACS Petrol. Chem. Div. Prepr. 38 (1993) 54–61.
[33] Y. Yoshimura, N. Matsubayashi, H. Yokokawa, T. Sato, H. Shimada, A. Nishijima, Ind. Eng. Chem. Res. 30 (1991) 1092–1099.
[34] Y. Yoshimura, Energy Fuels 8 (1994) 435–445.
[35] J. Bartholdy, P. Zeuthen, F.E. Massoth, Appl. Catal. A: Gen. 129 (1995) 33–42.
[36] P. Zeuthen, B.H. Cooper, F.T. Clark, D. Arters, Ind. Eng. Chem. Res. 34 (1995) 755–762.
[37] E. Furimsky, F.C. Massoth, Catal. Today 17 (1993) 537–666.
[38] F.T. Clark, M.C. Springman, D. Willcox, I.E. Wachs, J. Catal. 139 (1993) 1–18.
[39] R.J. Quan, R.A. Wane, C.W. Hung, J. Wei, Adv. Chem. Eng. 14 (1988) 95–257.
[40] D. Dong, S. Jeong, F.E. Massoth, Catal. Today 37 (1997) 267–275.
[41] E. Furimsky, Erdöl Kohle 35 (1982) 455–464.
[42] P. Zeuthen, P. Blom, F.E. Massoth, Appl. Catal. 78 (1991) 265–276.